Journal of Applied Electrochemistry **33**: 589–595, 2003.

γ-Butyrolactone-ethylene carbonate based electrolytes for lithium-ion batteries

A. CHAGNES[1], H. ALLOUCHI[1], B. CARRÉ[1], G. ODOU[2], P. WILLMANN[3] and D. LEMORDANT[1,*]
[1]*Laboratoire de Physico-chimie des Interfaces et des Milieux Réactionnels (EA2098), Faculté des Sciences, Parc de Grandmont 37200 Tours, France*
[2]*LDSMM (ESA8024), Université Lille 1, 59655 Villeneuve d'Ascq Cedex*
[3]*CNES, 18 Avenue E. Belin, 31055 Toulouse Cedex, France*
*(*author for correspondence, fax: +33 2 47 36 69 60, e-mail: lemordant@univ-tours.fr)*

Received 15 April 2002; accepted in revised form 5 February 2003

Key words: butyrolactone, conductivity, ethylenecarbonate, lithium batteries, organic electrolytes, viscosity

Abstract

γ-Butyrolactone-ethylene carbonate (BL-EC) mixtures have been investigated as electrolytes for Li-ion batteries using $LiPF_6$ and $LiBF_4$ as lithium salt. The thermal stability of the electrolytes in a large range of temperatures (−90 °C to 40 °C) have been studied by differential scanning calorimetry (DSC) and X-ray diffraction (XRD). From the results of these experiments, the phase diagram of the BL-EC system has been determined. It is characterised by a eutectic point at −56.3 °C and a molar fraction in EC: $x_{EC} = 0.1$. A metastable compound has been demonstrated below −90 °C at $x_{EC} = 0.4$. Conductivity measurements of BL-EC solutions, in the presence of $LiPF_6$ and $LiBF_4$, indicate that $LiPF_6$ in the eutectic mixture is the most conducting electrolyte in the range of temperatures investigated (−30 °C to room temperature). Nevertheless, at low temperature, $LiBF_4$ based electrolytes compete well with $LiPF_6$, especially when the amount of EC in the mixture is as high as $x_{EC} = 0.5$. Moreover, recrystallisation of the salt below −20 °C is avoided when $LiBF_4$ is used as salt. A large increase in viscosity of the solvent mixture is observed when a salt is added, but the increase is lower for $LiBF_4$ than $LiPF_6$. When EC is added to BL at constant salt concentration (1 M), the conductivity of $LiPF_6$ solutions decreases more rapidly than $LiBF_4$ solutions. This has been attributed, at least partially, to the dissociating power of EC. The electrochemical windows of BL-EC (equimolar) mixtures in the presence of $LiPF_6$ and $LiBF_4$ are comparable but it is shown that the solvents oxidation rate at high potentials is lower when $LiBF_4$ is used.

1. Introduction

Since the first battery marketed by Sony in 1990, Li-ion batteries have been improved in terms of volume, weight, specific energy and cycle life. Since this date, much research has focused on the search for new electrode materials. Another trend concerns the search for new electrolytes in order to enhance the passive layer at graphite electrodes [1], to clear up safety problems due to the flammability of organic electrolytes [2] and to improve ionic conductivity at low temperatures [3,4].

Some characteristics of lithium ion batteries, such as life time, specific power and good performance at low temperatures are largely dependent on the formulation of the electrolyte, which is generally composed of a mixture of solvents and a lithium salt. Military and space applications in particular require batteries which can operate at negative temperatures, generally down to −40 °C. To maintain the electrolyte in a liquid state at low temperatures, solvent mixtures exhibiting a low eutectic point are useful. For practical use in the field of Li batteries, the solvent mixture has to conform with the following requirements: a low viscosity (η) to enhance ionic mobility, a high permittivity (ε) for salt dissociation and a large electrochemical window to avoid gas formation and byproducts at the electrodes.

Butyrolactone (BL) is an interesting solvent, as it has a low melting point for low temperature applications, and a high boiling point [5]. Its permittivity is high enough to permit the dissociation of lithium salts having large anions bearing a delocalised charge such as $TFSI^-$ or PF_6^-. Generally, the BF_4^- anion leads to less conducting solutions as it is more associated in pairs than the preceding anions [6]. With the addition of a high permittivity cosolvent to BL, such as ethylene carbonate (EC), it is expected that, in spite of its high fusion point, the melting point will decrease by the formation of a eutectic mixture [7] and that the dissociation of the lithium salts will be enhanced,

leading to more conducting solutions. Another advantage to the use of EC as cosolvent is its excellent filming properties at the graphite anode leading to an improved cycling life [8–10].

Lithium hexafluorophosphate ($LiPF_6$) is widely used as lithium salt in carbonate based solvents as it exhibits a high conductivity and it is not aggressive toward metallic current collectors. Lithium tetrafluoroborate ($LiBF_4$) is less used as it leads to less conducting solutions than $LiPF_6$. Nevertheless, $LiBF_4$ has been used in primary lithium batteries and propylene carbonate (PC)-EC-BL based secondary Li-ion batteries [7].

2. Experimental details

BL (purity > 99.99%) and EC (purity > 99.99%) were obtained from Merck and used as received. $LiPF_6$ (99.99%), $LiBF_4$ (99.99%) were dissolved in the solvent or in the solvent mixture in a dry box. The water content of the solutions was less than 50 ppm as indicated by the manufacturer.

A.c. conductivity measurements were carried out using a conductivity cell equipped with platinum electrodes and a Philips PM6303 impedance analyser operating at 1000 Hz. Viscosity measurements were obtained using an Ubbelhode capillary tube immersed in a thermostated bath (±0.02 °C) and a Schott viscometer (AUS 310). The densities of the solutions, required to calculate the dynamic viscosities, were determined using picnometers.

DSC experiments were performed using 50 μL hermetically sealed aluminium cells containing a small volume of liquid (10–20 μL). The reference cell was filled with silica. Thermograms were recorded using a Perkin Elmer DSC 6 apparatus equipped with a nitrogen gas flow system cooled by liquid nitrogen. To prevent water condensation, a stream of nitrogen was continuously passed around the sample holder. The heating and cooling rates were fixed at 10 °C min^{-1}.

XRD investigations were performed with an INEL CPS 120 diffractometer using CuK_{α_1} radiation. Capillaries were sealed so that no hydration phenomenon occured during XRD investigations at low temperature. Samples were cooled by an Oxford system using nitrogen gas vapourized from the liquid contained in a cryogenic tank. The cooling rates in DSC and XRD are different and for this reason, the temperature of the sample measured during the XRD experiment was less precise (about ±10 °C) than during the DSC experiment (±1 °C).

The electrochemical windows of the prepared electrolytes were determined using a computerized EG&G potentiostat/galvanostat Versastat II. Lithium metal electrodes were used as reference and auxiliary electrodes. A platinum rotating electrode was used as working electrode to perform linear sweep voltametry.

3. Results and discussion

3.1. *Thermal stability*

3.1.1. *DSC experiments*

The phase stabilities of mixtures of organic solvents, used in the field of lithium batteries, have not been extensively examined. Recently, the phase diagram of mixtures of cyclic carbonates like EC, and linear carbonates such as dimethylcarbonate (DMC) or ethylmethylcarbonate (EMC), have been reported by Ding et al. [11]. According to these authors, the solvent systems studied do not exhibit phase transitions other than the melting of pure solid phases. The diagram is essentially characterized by a eutectic point whose composition lies close to the compound having the lowest melting point. Moreover, no miscibility gap is observed in the liquid state, nor mutual solubility in the solid state. In a previous paper [12], we have examined the thermal stability of the BL-DMC system, using differential scanning calorimetry (DSC) and X-ray diffraction (XRD) at low temperatures. Two polymorphs of BL with a monotropic transformation and two polymorphs of DMC with an enantiotropic transformation induced by BL were demonstrated. The BL-DMC diagram is characterized by a eutectic point at −57.5 °C and $x_{DMC} = 0.12$.

In this work, we analyse the thermal behaviour of BL-EC mixtures by DSC and XRD. DSC experiments were carried out at molar fractions in EC covering the whole range of compositions. Typical DSC curves were selected corresponding to $x_{EC} = 0.05$, 0.1, 0.4 and 0.9. Results are shown in Figure 1.

The thermogram reported in Figure 1(a), obtained for $x_{EC} = 0.05$, exhibits a sharp exothermic peak at −72.3 °C on the forward cooling scan corresponding to the crystallization of the subcooled liquid. On the reverse scan, a first exothermic peak is observed at −71.8 °C, which may correspond to the crystallization of amorphous domains formed during the forward cooling scan [13]. The glass transition preceding crystallization has not been observed on the DSC trace nor in the XRD experiment (see below). This exothermic peak is observed between $x_{EC} = 0.05$ and $x_{EC} = 0.4$, but not at higher content in EC. Two following endothermic peaks are observed on heating respectively at −56.3 °C and −41.7 °C. The first peak corresponds to the fusion of the eutectic mixture and the second to the fusion of the remaining solid BL.

The thermogram reported in Figure 1(b), obtained $x_{EC} = 0.1$, shows an exothermic peak at −72 °C on cooling, corresponding to the crystallization of the subcooled liquid. On the reverse scan, the fusion of the eutectic mixture occurs at −56.3 °C. As this is the exact composition of the eutectic, no other peaks are observed on further heating.

For $x_{EC} = 0.4$ (Figure 1(c)), the crystallization of the liquid mixture is noted as an exothermic peak at −70 °C on cooling. On the reverse scan, an exothermic broad

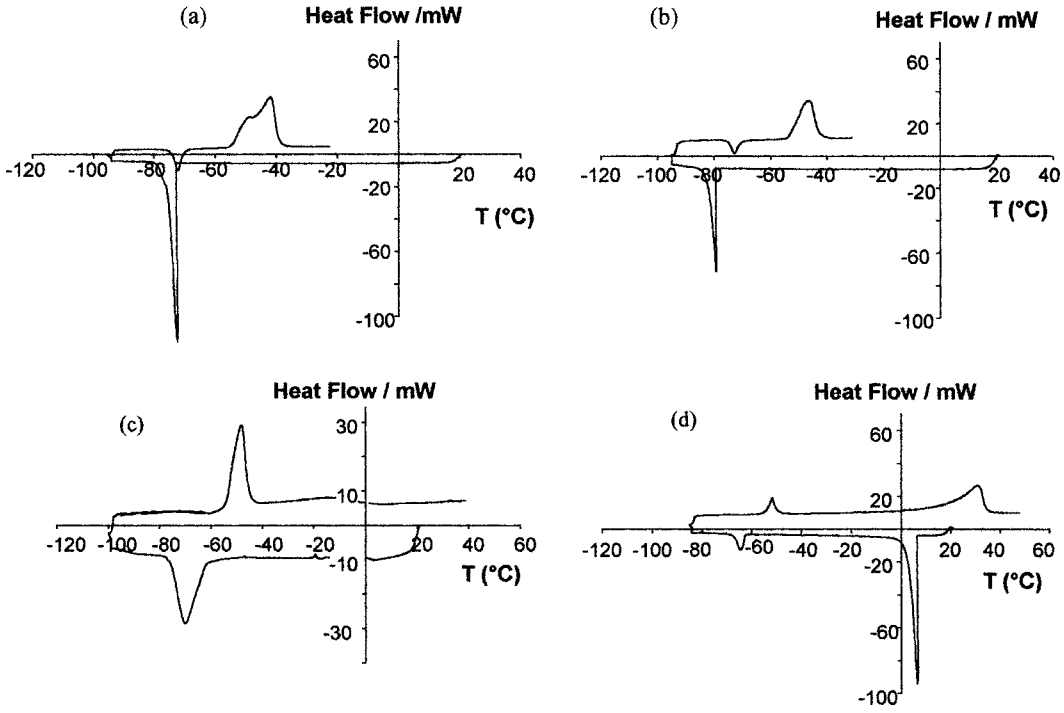

Fig. 1. DSC thermograms of the BL-EC mixtures for $x_{EC} = 0.05$ (a), $x_{EC} = 0.1$ (b), $x_{EC} = 0.4$ (c) and $x_{EC} = 0.9$ (d); endothermic upward.

peak is observed between −70 °C and −60 °C related to the recrystallization of the amorphous phase previously cited. The two following endothermic peaks, observed at −57.5 °C and −10 °C, correspond to the fusion of the eutectic mixture and the fusion of EC in excess.

For $x_{EC} = 0.9$ (Figure 1(d)), two exothermic peaks are observed, respectively, at 6.4 °C and −65.6 °C when the mixture is cooled. The first peak may be attributed to the crystallization of EC, the main component of the mixture, and the second peak to the crystallization of BL from the eutectic mixture. This crystallization occurs at a lower temperature than expected from the preceding experiments for an unknown reason. On the reverse scan, the fusion of the eutectic mixture occurs at −55.6 °C and the fusion of EC is achieved at 31.5 °C.

3.1.2. *XRD experiments*

To confirm the preceding observations, XRD experiments were carried out on BL-EC mixtures having the following compositions in EC: $x_{EC} = 0.05$, 0.4 and 0.9. The results and XRD spectra of BL and EC are reported, respectively, in Figures 2, 3 and 4.

The XRD spectra displayed in Figure 2 ($x_{EC} = 0.05$) correspond to a mixture of two solid phases (BL and

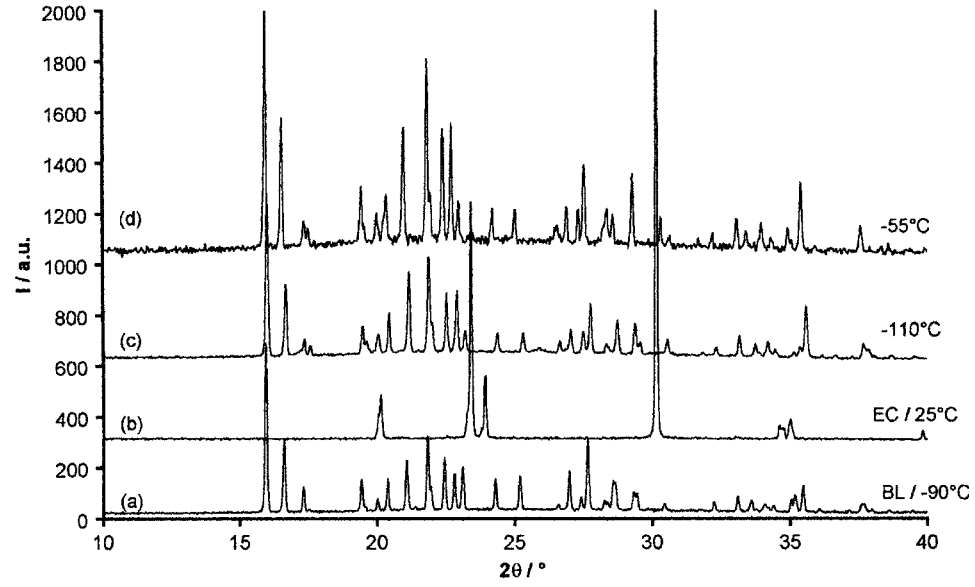

Fig. 2. XRD pattern of BL at −90 °C (a), EC at 25 °C (b) and BL-EC ($x_{EC} = 0.05$) at −110 °C (c) OR −55 °C (d).

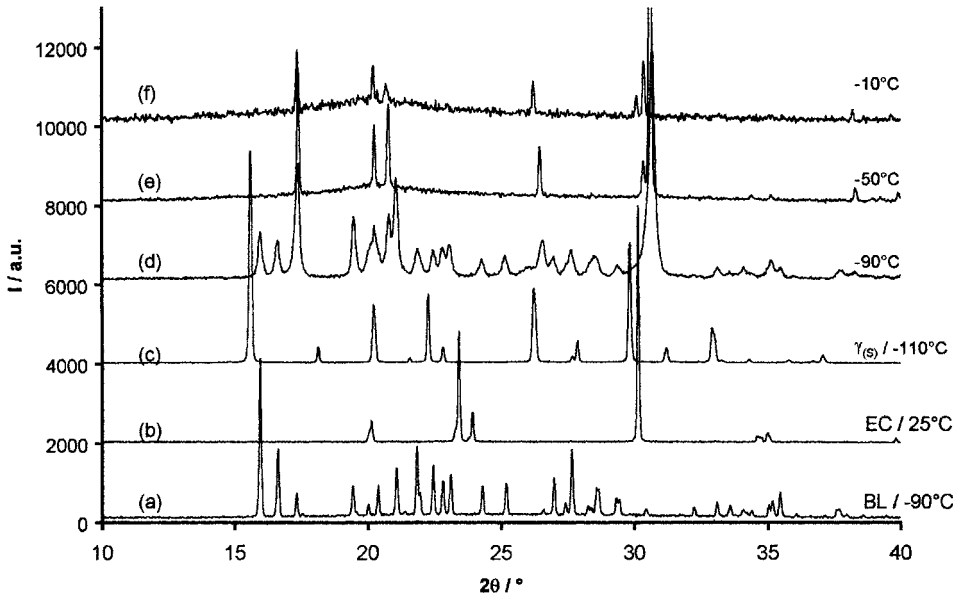

Fig. 3. XRD pattern of BL at −90 °C (a), EC at 25 °C (b) and BL-EC ($x_{EC}=0.4$) at −110 °C (c) OR −90 °C (d), −50 °C (e) OR −10 °C (f).

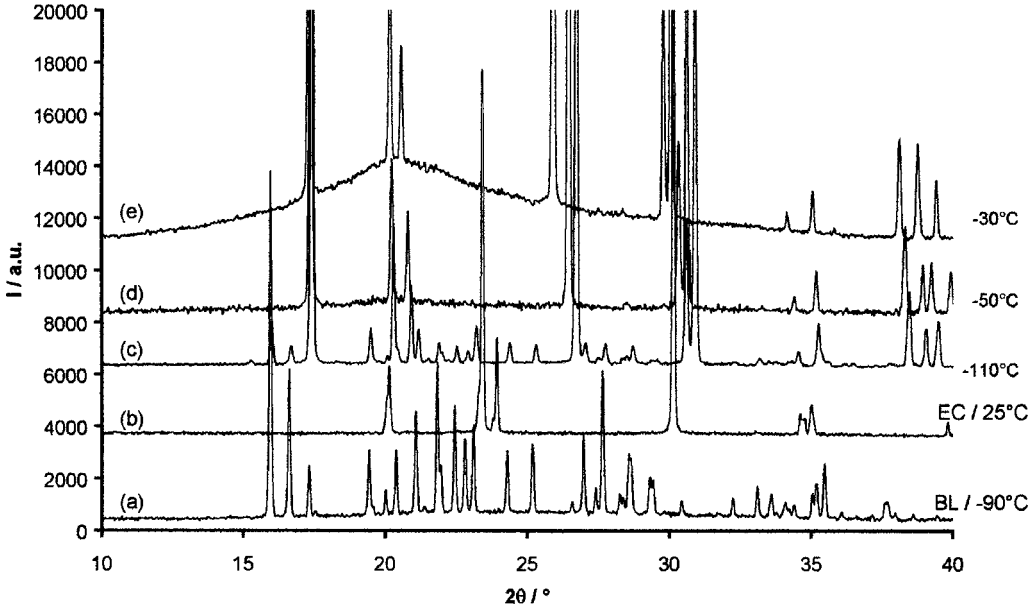

Fig. 4. XRD pattern of BL at −90 °C (a), EC at 25 °C (b) and BL-EC mixtures at −110 °C (c), −50 °C (d) or −30 °C (e).

EC). No phase transition, other than the fusion of the solid phases, occurs between −110 °C (Figure 2(c)) and −55 °C (Figure 2(d)). The curvature of the base-line observed at −55 °C (Figure 2(d)) shows the presence of the liquid eutectic phase.

The XRD spectrum reported in Figure 3(c), for $x_{EC} = 0.4$, indicates the presence of a metastable compound at −110 °C which disappears between −110 °C and −90 °C (Figure 3(d)). The presence of this metastable compound has not been detected by DSC as it is formed at lower temperature than the cooling capability of the DSC apparatus. The spectrum obtained at −90 °C (Figure 3(d)) corresponds to a complex mixture of the metastable compound, solid BL and EC. Liquid eutectic and remaining solid EC appear at −50 °C (Figure 3(e)). Fusion of EC is achieved at temperatures above −10 °C as seen on the XRD pattern reported in Figure 3(f).

The XRD spectrum of the BL-EC mixture with $x_{EC} = 09$ is displayed in Figure 4. At the lowest temperature (−110 °C, Figure 4(c)), a mixture of two solids (BL + EC) appears. At −50 °C (Figure 4(d)), the remaining spectrum corresponds to solid EC and at −30 °C (Figure 4(e)), the amount of liquid phase increases owing to the fusion of EC.

By means of the DSC and XRD investigations, it is possible to establish the phase diagram of the BL-EC system. As shown in Figure 5, the phase diagram is characterized by an eutectic point located at $x_{EC} = 0.1$

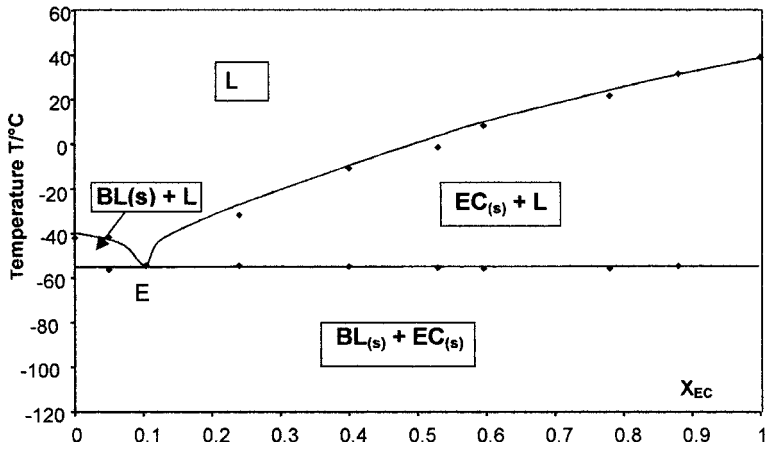

Fig. 5. Phase diagram of BL-EC mixtures (L: liquid).

and $T = -56.3$ °C. The metastable compound, shown at low temperatures in XRD experiments for $x_{EC} = 0.4$, has not been reported on the diagram relative to stable phases. As a consequence, the $x_{EC} = 0.1$ BL-EC mixture appears to be the most interesting formulation for thermal stability. According to its fusion point, this mixture remains liquid beyond −56.3 °C without adding salt.

3.2. *Viscosity*

In Figure 6, viscosity variations have been plotted against the temperature for two BL-EC mixtures ($x_{EC} = 0.2$ and $x_{EC} = 0.5$) in the absence of salt and for $x_{EC} = 0.5$ in the presence of $LiPF_6$ and $LiBF_4$ at a concentration of 1 mol L^{-1} (1 M). The viscosities of the two solvent mixtures with and without salts are reported in Table 1. The activation energies $E_{a,\eta}$ for the viscous flow, deduced from the dependency of η on the temperature, according to the Eyring's theory for activated processes [14]:

$$\eta = hN_a/V_m \exp(\Delta S^{\neq}/R) \times \exp(\Delta H^{\neq}/RT) \quad (1)$$

are reported in Table 1. In Equation 1, h is the Planck constant, V_m the molar volume of solvent, $\Delta S^{\neq}$ and $\Delta H^{\neq}$, the activation entropy and enthalpy for flow process, respectively. In condensed phases, $\Delta H^{\neq}$ represents the activation energy of the viscous flow $E_{a,\eta}$, which is readily obtained from the slope $(\Delta H^{\neq}/R)$ of the curve representing the variations of Ln η against $1/T$.

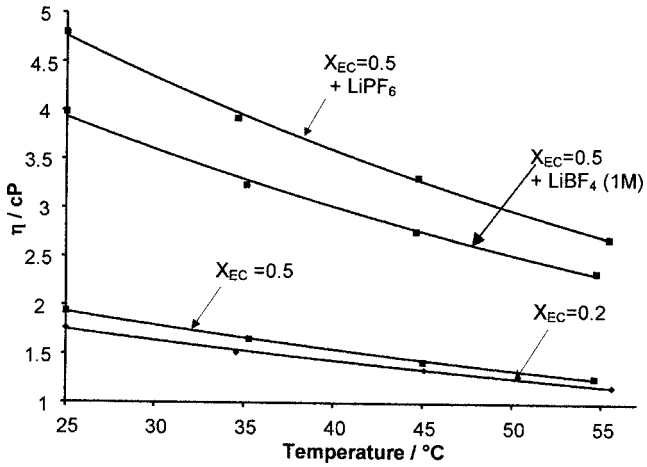

Fig. 6. Variations of the viscosity of BL-EC mixtures ($x_{EC} = 0.2$ and $x_{EC} = 0.5$) + $LiPF_6$ (1 M) or $LiBF_4$ (1 M) with the temperature.

As expected, the viscosity increases with the molar fraction in EC but, in the absence of salt, the viscosity is practically independent of the mixture composition in the range $x_{EC} = 0$ to $x_{EC} = 0.5$, at all the temperatures investigated. In the presence of $LiPF_6$ or $LiBF_4$, the viscosities of the $x_{EC} = 0.5$ solvent mixture increase drastically. $LiPF_6$ leads to more viscous solutions than $LiBF_4$, owing to the different size of PF_6^- and BF_4^-.

3.3. *Conductivity*

In Figure 7, the conductivities at 25 °C of BL-EC electrolytes containing $LiPF_6$ (1 M) and $LiBF_4$ (1 M) are plotted against the molar fraction in EC. The

Table 1. Viscosity and activation energy for the viscous flow at 25 °C of BL-EC mixtures with or without added salts

x_{EC}	BL/EC		BL/EC + $LiPF_6$(1 M)		BL/EC + $LiBF_4$ (1 M)	
	η /cP	$E_{a,\eta}$ /kJ mol^{-1}	η /cP	$E_{a,\eta}$ /kJ mol^{-1}	η /cP	$E_{a,\eta}$ /kJ mol^{-1}
0.2	1.77	10.7	–	–	–	–
0.5	1.94	11.8	4.79	15.2	3.98	14.3

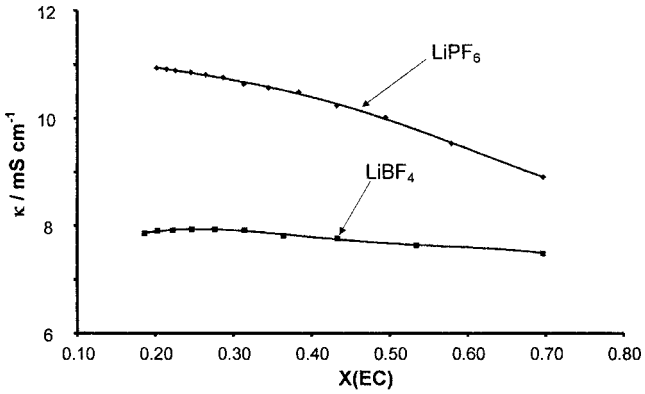

Fig. 7. Variation of the conductivity at 25 °C of BL-EC electrolytes containing $LiPF_6$ (1 M) or $LiBF_4$ (1 M) with the molar fraction in EC.

conductivities of the $LiPF_6$ based electrolytes decrease steadily when the content in EC increases in the mixture but the conductivities of $LiBF_4$ based electrolytes remain approximately constant. The behaviour of $LiBF_4$-based electrolytes is due to the fact that, in BL, this salt is partially associated as ion pairs [15]. The addition of EC, which has a high dielectric constant, promotes the dissociation of $LiBF_4$ pairs into free ions leading to an increase in the number of charge carriers. This compensates the increase in viscosity and, hence, the decrease in mobility which occurs when the content in EC increases. In $LiPF_6$-based electrolytes, the increase in viscosity is mainly responsible for the observed decrease in conductivity because this salt is already fully dissociated in BL [4, 16]. The addition of EC to BL will increase simultaneously the dielectric constant and the viscosity of the mixture.

In terms of conductivity at room temperature or higher temperatures, the $LiPF_6$-based electrolytes are more interesting for practical applications. At low temperatures, however, $LiBF_4$-based electrolytes could compete with $LiPF_6$-based electrolytes. In Figure 8, the conductivities of the two solvent mixtures ($x_{EC} = 0.1$ and $x_{EC} = 0.5$) in the presence of $LiPF_6$ (1 M) and $LiBF_4$ (1 M) have been plotted against the temperature in the range +20 °C to −40 °C. When $LiPF_6$ is used as salt, the curve representing the conductivity of the BL-EC ($x_{EC} = 0.5$) electrolyte exhibits sudden drop around −20 °C. This has been attributed to a partial recrystallization of $LiPF_6$ in the solvent mixture induced by the stirring during the conductivity measurements. In fact, when no stirring is performed, no phase transition is observed during the DSC experiment with this electrolyte.

The conductivities at −20 °C are reported in Table 2 for comparison. It is shown that, below −10 °C, the conductivities of $LiBF_4$-based electrolytes are of the same order of magnitude as those of $LiPF_6$ and that the occurrence of recrystallization is avoided.

3.4. *Electrochemical window*

The electrochemical window of the $LiPF_6$ and $LiBF_4$-based electrolytes in BL-EC ($x_{EC} = 0.5$) have been determined at a platinum rotating disc electrode (rotating speed 1000 rpm) and at a scan rate of 5 mV s^{-1}. The voltammograms reported in Figure 9 show that the oxidation potential of these electrolytes occurs at a potential of 5.5 V vs Li^+/Li in the range of the current densities used. Beyond 5.5 V, the oxidation rate of the solvent mixture is clearly lower in the presence of $LiBF_4$. However, the electrochemical window of both electrolytes is large enough for their use in the field of lithium ion batteries.

Table 2. Conductivity (in mS cm^{-1}) of $LiPF_6$ and $LiBF_4$ in BL-EC electrolytes at −20 °C and activation energy for the conductivity

x_{EC}	BL-EC + $LiPF_6$ (1 M)	BL-EC + $LiBF_4$ (1 M)
0.1	3.15	2.86
0.5	2.62	2.37

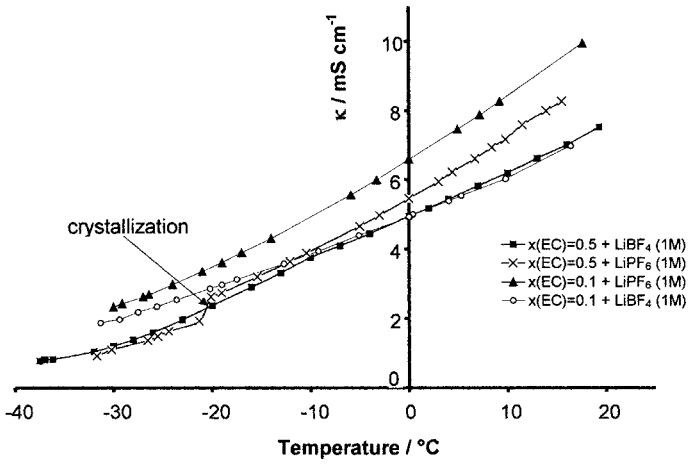

Fig. 8. Variation of the conductivity of BL-EC ($x_{EC} = 0.5$ and $x_{EC} = 0.1$) electrolytes containing $LiPF_6$ (1 M) or $LiBF_4$ (1 M) with the temperature.

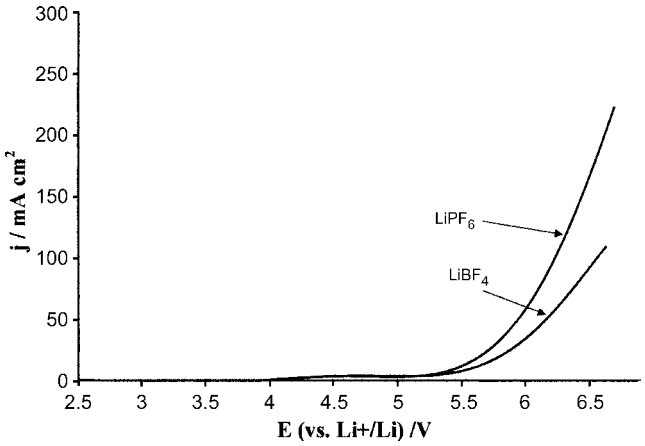

Fig. 9. Electrochemical window of BL-EC ($x_{EC} = 0.5$) electrolytes containing $LiBF_4$ (1 M) or $LiPF_6$ (1 M).

4. Conclusion

Precise knowledge of the thermodynamic stability and relationships between different solid phase of a solvent mixture system is a prerequisite for understanding the crystallization process and, hence, the thermal stability of an electrolyte. Phase diagrams of temperature versus composition at constant pressure for binary systems give useful information about the temperature of liquid–solid transition, even if the binary phase diagram is slightly modified in the presence of the salt. The phase diagram of the BL-EC system exhibits an eutectic point at $x_{EC} = 0.1$ and $T = -56.3$ °C. As indicated by DSC and XRD experiments, no stable solid compound other than the pure solvents are formed in the range of temperatures investigated.

Conductivity and viscosity studies of $LiPF_6$ and $LiBF_4$ solutions in the eutectic BL-EC and the equimolar solvent mixture indicate that the most conducting solutions at room temperature or higher are obtained with $LiPF_6$, but that below −10 °C the conductivities of $LiBF_4$-based electrolytes are of the same order of magnitude as those of $LiPF_6$. Moreover, the thermal stability of $LiBF_4$-based electrolytes is higher as no recrystallization occurs. Viscosity studies indicate that the addition of EC to BL leads to an increase in the number of charge carriers in the case of $LiBF_4$, but not to an increase in conductivity owing to the increase in viscosity of the solvent mixture. The electrochemical windows of $LiPF_6$ and $LiBF_4$ BL-EC electrolytes are similar, but the oxidation current at high applied potential ($E > 5.5$ V vs Li^+/Li) is higher in the case of $LiPF_6$.

Acknowledgement

A. Chagnes would like to express thanks to Région Centre for financial support.

References

1. G.-C. Chung, *Electrochem. Commun.* **1** (1999) 493.
2. S.-I. Tobishima and J.-I. Yamaki, *J. Power Sources* **81** (1999) 882.
3. A. Chagnes, B. Carré, P. Willmann and D. Lemordant, *Electrochim. Acta* **46** (2001) 1783.
4. A. Chagnes, B. Carré, P. Willmann and D. Lemordant, *J. Power Sources* **109** (2002) 203.
5. R. Naejus, D. Lemordant and R. Coudert, *J. Chem. Thermodyn.* **29** (1997) 1503.
6. A. Moumouzia and G. Panapoulos, *J. Chem. Eng. Data* **36** (1991) 20.
7. M. Winter and J.O. *Besenhard, in* M. Wakihara and O. Yamamoton (Eds), '*Lithium Ion Batteries*: *Fundamentals and Performance*', (Wiley–VCH, New York, 1999).
8. J.O. Besenhard and H.P. Fritz, *J. Electroanal. Chem.* **53** (1974) 329.
9. J.O. Besenhard, M. Winter, J. Yang and W. Biberacher, *J. Power Sources* **54** (1995) 228.
10. M.C. Smart, B.V. Ratnakumar and S. Surampudi, *J. Electrochem. Soc.* **146** (1999) 486.
11. M.S. Ding, K. Xu and T.R. Jow, *J. Electrochem. Soc* **147** (2000) 1688.
12. M.S. Ding, K. Xu and T.R. Jow, *J. Electrochem. Soc.* **148** (2001) A299.
13. A. Chagnes, B. Carré, V. Agafonov, P. Willmann and D. Lemordant, *J. Phys. IV*, 11 (Pr 10, XXVII JEEP, *Journées d'Etude des Equilibres entre Phases* 2001) 27.
14. D. Giron, *Electrochim. Acta* **248** (1995) 1.
15. J.F. Kincaid, H. Eyring and A.E. Stearn, *Chem. Rev.* **28** (1941) 301.
16. K. Hayamizu, *Solid State Ionics* **107** (1998) 1.
17. I. Geoffroy, P. Willmann, K. Mesfar, B. Carré and D. Lemordant, *Electrochim. Acta* 45 (2000) 2019.